In-Vehicle PLC Simulator Based on Channel Measurements

Philippe Tanguy and Fabienne Nouvel
Institute for Electronics and Telecommunications of Rennes (IETR) - UMR CNRS 6164
INSA 20 avenue des Buttes de Coësmes,
CS 70839, 35708 Rennes cedex 7, France.
Email: philippe.tanguy@insa-rennes.fr

***Abstract*—This paper deals with the in-vehicle networks. We propose to study a network which does not need new wires based on Power Line Communication (PLC). Indeed, the automotive communication networks have evolved and the electronic devices in-vehicle are widespread. It appears that with the increase of electronic devices there is a wire harness bottleneck. So, PLC seems to be a promising in-vehicle networks for high data rates applications. In-vehicle PLC channels and background noise measurements are presented. We discuss the PHY layer PLC system simulator based on these measurements.**

I. Introduction

Recently the definition of IEEE P1901 draft standard for broadband over power line communications (PLC) and networks has been approved. It covers both the medium access control and the physical layer specifications. Moreover, the PLC technology is nowadays adopted in many AC indoor applications. The re-use of in-vehicle power lines for data transmissions seems to be an attractive and alternative solution as for indoor.

In fact, modern cars have more and more electronic control units (ECU) which need more and more buses for exchanges. So, PLC in-vehicle can avoid the weigthed growth of wire harnesses.

One first idea may be to adapt indoor PLC devices for in-vehicle communications. In previously research [1] different indoor PLC standards have been study in-vehicle. Moreover, in [2] two high data rate PLC indoor modems have been studied. The obtained data rates ($[10-20]\ Mbps$) seem to be very promising compare to existing field buses in comparison with the FlexRay protocol that has a maximum data rate of 10 Mbps. However, PLC indoor standard cannot be adapted directly for vehicle. Furthermore, the EMC requirements must be matched.

Developing PLC in-vehicle systems requires the knowledge of the propagation channel. The channels have been studied previously and results show that they are frequency selective [3], [4]. In addition, the impulsive noise seems to be one of the most important perturbation in PLC system as prestented in [5], [6] and [7].

This paper is dedicated to channel and background noise measurements in order to develop an in-vehicle PLC simulator based on in-vehicle channels measurements.

In next section, we provide details about the measurements setup. Section II-A deals with channel measurements as II-B deals with background noise measurements. Then, in section III, we introduce our system simulator where we compute the theoretical capacity. The conclusion is given in section IV.

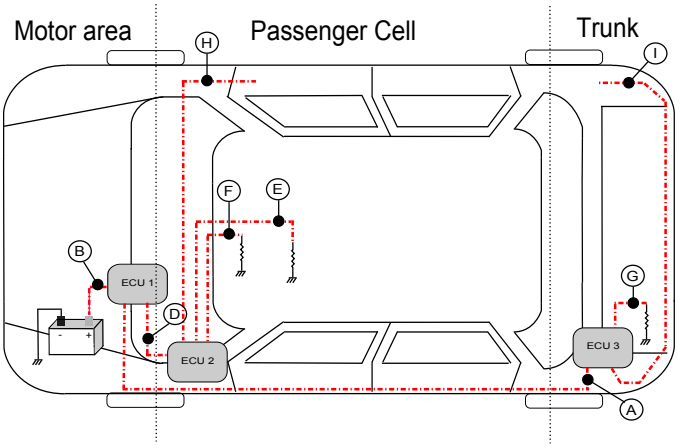

Fig. 1. Scheme of the car Peugeot 407 SW. The different uppercases represent the measurement points.

II. Channel measurement

We perform measurements on various paths between two ECUs in a vehicle in order to analyze the propagation channel and to integrate the measurements in the simulator. All of them are carried out through a PLC coupler with a reference impedance of $50\ \Omega$. The coupler consists on a capacitance and a HF transformer that has an attenuation lower than $0.5\ dB$ in the bandwidth $[4-30]\ MHz$.

The main contribution here is the channel measurements during a continuous time in order to analyze the variations while driving (vehicle in motion and equipments connected to DC line).

A. S-parameters measurements

1) Testbed: Fig. 1 presents the location of the measurement points. The S-parameters are recorded using a full 4 ports Vector Network Analyzer (VNA) and a PC interfaced with the VNA. We measure the S-parameters during about 10 minutes while the car is moving. The S-parameters (GF-GH-HD) are registered about every 10 seconds for the 3 different paths. We can notice that both points G and F are cigar lighters.

TABLE I
VECTOR NETWORK ANALYSER PARAMETERS

Parameters	values
Start frequency	1 MHz
Stop frequency	31 MHz
RBW	10 KHz
Points acquired	1001
Sweep time	single

TABLE II
COHERENCE BANDWIDTH GF, GH AND HD PATHS

	min	max	mean	std
$BC_{0.9}$ GF	419 KHz	659 KHz	502 KHz	66 KHz
$BC_{0.9}$ GH	599 KHz	839 KHz	702 KHz	53 KHz
$BC_{0.9}$ HD	1.6 MHz	1.9 MHz	1.8 MHz	83 KHz

The VNA can record the 4 S-parameters. In fact the VNA is a 2 ports bidirectional analyzer, thus it can capture S_{12} and S_{21} parameters nearly simultaneously. The S-parameters used for the measurements are described in the Table I. We can notice that the calibration of the 4 ports of the VNA has been realized with the cables and without the couplers. These parameters will be used to compute the coherence bandwidth and the RMS time delay.

2) Statistical analysis: The coherence bandwidth is given by the autocorrelation function of S_{21} parameters [8]

$$R(\Delta f) = \int_{-\infty}^{+\infty} H(f)H^*(f+\Delta f)df \tag{1}$$

where H denotes the complex coefficient S_{21} from the VNA. In the time domain thanks to the impulse response the propagation channel can be also characterized with the τ_{rms} which allows to have a measure of the delay spread. The RMS time delay spread is defined as

$$\tau_{rms} = \sqrt{\int_0^{\tau_m} (t-\tau_e-\tau_a)^2 P(t)dt}. \tag{2}$$

First introduce the τ_m parameter which is defined as the excess delay when the power delay profile $P(\tau)$ is under X_{dB} of the first arrival delay with

$$P(\tau) = \frac{|h(t)|}{\int_{-\infty}^{+\infty} |h(t)|^2 dt}. \tag{3}$$

We have decided to choose a reference attenuation of 30 dB in order to define the maximum excess delay. τ_a is defined like the first arrival path and τ_e like the first moment of the power delay profile

$$\tau_e = \int_0^{\tau_m} (t-\tau_a)P(t)dt. \tag{4}$$

The results of the coherence bandwidth and the RMS time delay spread are shown in Table II and III. The statistical analysis has been realized on 3 different paths and 60 measurements for each path.

TABLE III
TIME DELAY SPREAD GF, GH AND HD PATHS

	min	max	mean	std
τ_{rms} (GF)	174.7 ns	286.6 ns	252.6 ns	25.3 ns
τ_{rms} (GH)	116.2 ns	157.3 ns	138.7 ns	10.3 ns
τ_{rms} (HD)	51.7 ns	70.5 ns	62.5 ns	3.8 ns

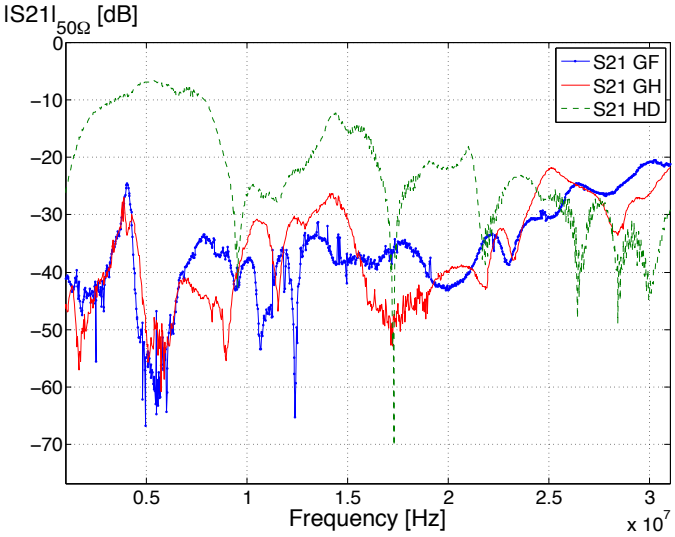

Fig. 2. S_{21} 3 paths: GF, GH and HD.

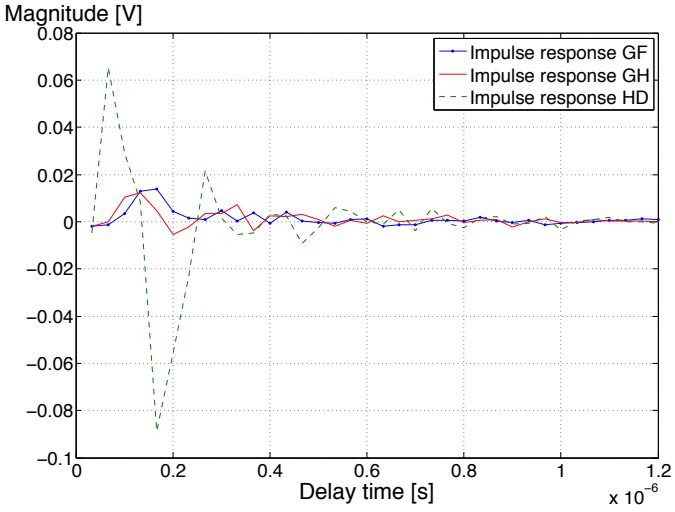

Fig. 3. Impulse Response 3 paths: GF, GH and HD.

3) Results and discussion: In Fig. 2 we show an example of 3 measurements of S_{21}. Fig. 3 represents three impulse responses calculated from the complex S_{21} parameter. The impulse response is calculated by the inverse Fourier transform of the S_{21} parameter. The curves in Fig. 3 exhibit some peaks which confirm the multi-paths PLC channel.

In Table II we can observe that the coherence bandwidth is between 419 KHz and 1.9 MHz. We remark that for the path HD the mean of coherence bandwidth is higher than the path GF and GH. As a result the topology for the path HD is better

TABLE IV
AVERAGE ATTENUATION OF GF, GH AND HD PATHS

Average attenuation of S_{21}	min	max	mean	std
GF (dB)	20.8	59.2	36.2	8
GH (dB)	20.9	55.8	36.2	8.7
HD (dB)	6.6	48.7	21.7	9.2

than the others. In Table III, we can observe the result of the time delay spread and we see that the min RMS delay spread is $51.7\ ns$ for the path HD and a maximum of $286.6\ ns$, for the path GF, which is five times longer than the first one.

In Table IV, we oberve the average attenuation of the paths GF, GH and HD. There is about about $15\ dB$ between HD and GF, and GH for the mean values. With this feature we can achieve a first classification of the channels for simulation study and defined use case. In fact, the path HD will be a channel identified as "Best Case" and the GH, and GF will be "Worst Case".

In a previous study on in-vehicle PLC, the authors in [3] find delay spread under $380\ \mu s$ and a coherence bandwidth greater than $400\ KHz$. To compare with indoor results we can mention the result of [8] where the minimum observed coherence bandwidth is $32.2\ KHz$ and the mean value of the RMS delay spread is $0.413\ \mu s$.

With this VNA we can compare the symmetry of the channel, i.e. compare S_{21} and S_{12}. We made the same comparison that in [4] and we take into account also that the transfer function S_{21} and S_{12} are identical.

B. Background Noise: Frequency Domain Measurement

In order to have a first evaluation about PLC data rate, we have measured the background noise over in-vehicle DC lines. In previous work [9] the background noise has been measured in several locations in the car and it can be seen that according to the location the parameters of noise are not the same. We have also decided to compare two type of measurements, one in the frequency domain with a spectrum analyzer and the other in the time domain with a digital storage oscilloscope (DSO).

1) Testbed: The background noise has been measured with a spectrum analyzer linked with a PC which remotes the device. The spectrum analyzer is connected to the DC line with the same coupler used for S-parameters measurements. As previously, 60 acquisitions have been performed every 10 seconds. Table V summarizes the parameters of the background noise measurement with the spectrum analyzer.

2) Results and discussion: Fig. 4 illustrates the measured background noise at 4 different points in the car. We measure the instantaneous power of background noise. Because of the system measurement we cannot see the difference between the power of background noise with and without presence of impulsive noise. Moreover, there is a delay of measurement because of the sweep time of the measurement. So, if the duration of an impulsive noise is lower than the sweep time we can have an effect of a part of the impulsive noise. It is also possible to have the contribution of two impulsive noises

TABLE V
BACKGROUND NOISE MEASUREMENTS: SPECTRUM ANALYZER PARAMETERS

Parameters	values
Start frequency	$0\ MHz$
Stop frequency	$50\ MHz$
Detection	RMS
RBW	$10\ KHz$
Trace mode	Normal
Nb points	501
Sweep time	$min = 10\ \mu s$

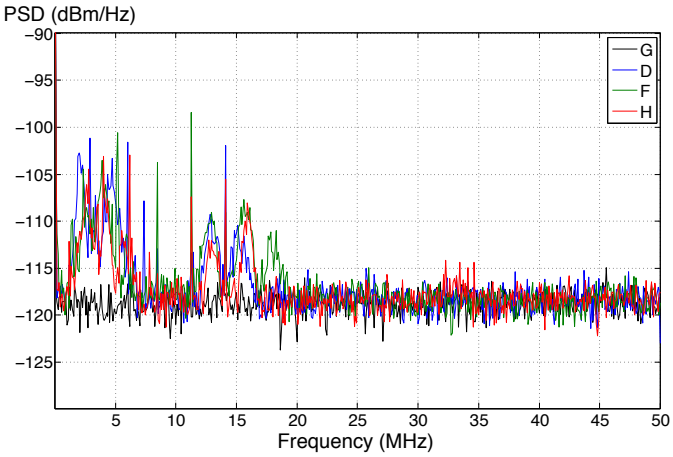

Fig. 4. Background noise 4 points: G, D, F, H

with an inter-arrival time lower than the sweep time. However, a spectrum analyzer has a better sensibility than DSO.

We observe that the background noise is different according to the location in the vehicle. We observed narrowband interferences in the bandwidth $[0-15]\ MHz$ for points D, F and H which are located in the front of the vehicle. We notice the presence of continuous interferences during the 60 recordings.

C. Background Noise: Time Domain Measurement

1) Testbed: For the measurement in time domain we have used a DSO. Like the device has 4 channels we have decided to make an acquisition on two channels in order to see the behavior of background noise at two points of a transmission path (between the transmitter and the receiver). We record $80\ ms$ of signal on the 2 channels with a sampling frequency of $100\ MS/s$ and a DAC (Digital Analog Converter) resolution of $8\ bits$.

2) Results and Discussion: Fig. 5 illustrates the measured background noise in the time domain. Here the path GF and the measurement at point G is presented. To compute the spectrogram we have decided to integrate some parameters of HPAV (HomePlug Av) standard. Hence, the spectrogram has been computed with the short Fourier transform, an Hamming window of length equal to the length of HPAV OFDM symbol ($40.96\ \mu s$) and an FFT size of 3072 points like in HPAV standard.

We observe an increase of background noise for some frequencies in the bandwidth $[0-5]\ MHz$. We remark that

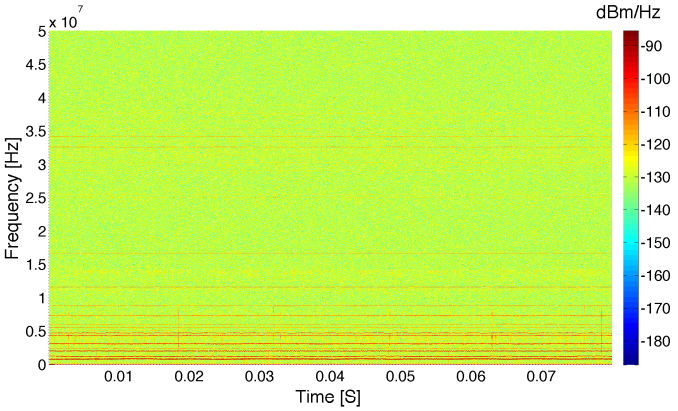

Fig. 5. Spectrogram at point G. Short Fourier transform of a signal of 80 ms recorded by a DSO. Sampling frequency: 100 MS/s.

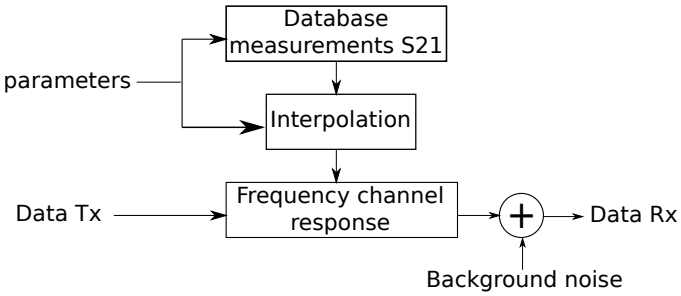

Fig. 6. Channel simulator.

the noise is localized in frequency and constant during the time of the recording. Therefore if OFDM modulation is used in this bandwidth several subcarriers will be affected by the noise during all the transmission time. Moreover, we can also observe an increase of noise for several frequencies but localized in time which can be explained by impulsive noise.

III. Channel simulator

In Fig. 6 we show the scheme of the channel simulator. Background noise and transfer function can be different according to the path in-vehicle but also according to the vehicle and its topology. Like vehicles have not the same electrical topology, the number of ECU, so the same number of loads on the electrical network and the same dimension we can not identify a particular channel model for simulation. However, the measurements are sufficient to be integrated in our channel simulator and to verify PHY layer parameters.

A. Transfert function: using measurement

We made several measurements of S_{21} and S_{12} in order to use it in our channel simulator. Because we have considered the channel like symmetric we can introduce in the channel simulator only the S_{21}. We use for the simulation the frequency transfer function. The simulation considers that there is no inter carrier interference (ICI) and intersymbol interference (ISI) because we made the hypothesis that the cyclic prefix (CP) has perfectly counteract the multi-path channel effects of the propagation channel. Moreover, we consider that the

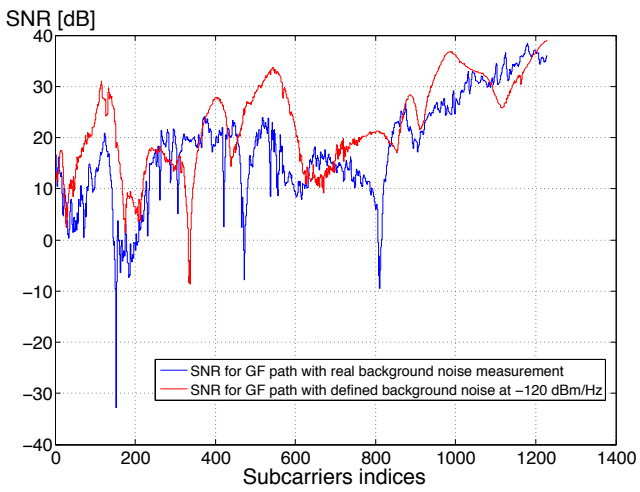

Fig. 7. SNR versus subcarrier indices for the path GF with two type of background noise: a defined background noise level at -120 dBm/Hz and a real measurement of the background noise at point F.

channel is time invariant. The data received at the output of the channel simulator are expressed by

$$y_i[n] = H_i[n]x_i[n] + \eta_i[n] \tag{5}$$

with $y_i[n]$ the symbol received, $H_i[n]$ the complex channel coefficient, $x_i[n]$ the QAM symbol to transmit, $\eta_i[n]$ the AWGN noise, nth QAM symbol and ith subcarrier.

B. Background noise

Indoor PLC communication defined several classes of noise. The background noise is generally not considered as AWGN. In fact, in indoor PLC the background noise is colored and decrease with the frequency. In order to take into account the background noise, it has been decided to consider the background noise has AWGN and for the level of noise the worst case has been chosen. In [10] the background has been measured while the car is moving. Degardin *et al.* conclude that the background noise can be modeled by an AWGN noise with a power spectral density $PSD = -130$ dBm/Hz. In [4] the background noise has been also measured at different points in a car. Mohammadi *et al.* find a background noise level between $PSD = -130$ dBm/Hz and $PSD = -120$ dBm/Hz.

In a first time, the AWGN noise will be used in our simulator. However, in Fig. 7 we propose to observe the difference of SNR when two type of background noise are chosen. The first type of background noise is an estimation of the background noise level at -120 dBm/Hz (AWGN noise). The second type is the real background noise measurements. We remark a lower SNR when the second type of background noise is introduced.

C. Capacity with the channel simulator

In this section, we verify the capacity of the channel for different paths and for a multi-carrier system. We have computed the capacity of the 60 transfer functions recorded

TABLE VI
SIMULATION PARAMETERS: FFT/IFFT AND Δ_f VALUES ARE PARAMETERS USED BY THE HPAV STANDARD

Parameters	values
Fmin	$1\ MHz$
Fmax	$31\ MHz$
Subcarrier	$N = 1228$
FFT/IFFT	3072
Δ_f	$24.414\ KHz$
PSD of noise (P_N)	$-120\ dBm/Hz$
PSD of signal (P_e)	$-60\ dBm/Hz$

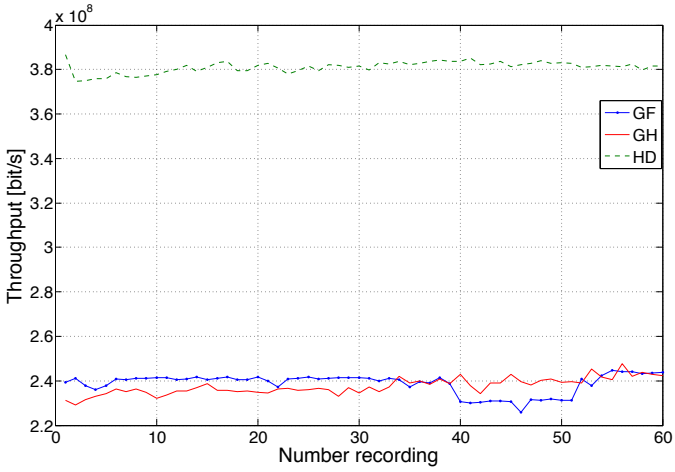

Fig. 8. Theoretical capacity; 3 paths: GF, GH, HD.

every $10\ s$ for the three paths. To compute the capacity, we have used

$$C = \Delta f \times \sum_{i=0}^{N-1} log_2(1 + SNR_i) \quad (6)$$

with $SNR_i = \frac{|H_i|^2 \times P_e}{P_N}$ the signal to noise ratio per subcarrier where P_e is the PSD of the emitted signal and P_N is the PSD of the background noise. In Table VI we show the simulation parameters which have been chosen to be like the parameters of HPAV standard. For the reasons developed in [10] we choose a PSD of $-60\ dBm/Hz$ for the signal injected in the DC lines.

D. Results and discussion

Fig. 7 shows that the SNR with real measurement of background noise is lower than AWGN model. In order to have a more realistic channel simulator, it will be good to integrate background noise model and impulsive noise model. But other measurements with different vehicles must be performed.

Fig. 8 illustrates the theoretical capacity versus time recording of S-parameters for 3 different paths. We observe that the capacity for the 3 paths are between $225\ Mbps$ and $386\ Mbps$. The throughput of HD is best because the average attenuation of this path in the bandwidth considered is better than the others for this vehicle. If we compare with previously work [2], we can notice that we have the same trends. In fact, the path HD is better than GH and GF. Moreover, the capacity has small variation during the measurement time.

IV. CONCLUSION

A campaign of measurements has been realized in order to use the results in a channel simulator directly. We have compute the channel capacity and with the parameters of simulation we can observe a minimum capacity of about $225\ Mbps$. In future work it can be interesting to define use cases in order to test simulation link of PHY layer. Indeed, it can be interesting to distinguish worst case and best case. The use cases can be separate according to several features like the capacity, the level of background noise or the average channel attenuation for example. Finally, an important way for simulation of PLC in-vehicle communications is the integration in the study of impulsive noise which will be part of the next measurements.

ACKNOWLEDGMENT

This work has been carried out by the CIFAER project, initiated and supported by the ANR and by the French Premium Cars Competitiveness Cluster ID4car.

REFERENCES

[1] F. Nouvel and P. Maziero, "X-by-wire and intra-car communications: power line and/or wireless solutions," in *Proc. IEEE Intl. Conference on Intelligent Transport Systems Telecommunications*, Oct. 2008, pp. 443–448.

[2] P. Tanguy, F. Nouvel, and P. Maziero, "Power Line Communication standards for in-vehicle networks," in *Proc. IEEE Intl. Conference on Intelligent Transport Systems Telecommunications*, Oct. 20-22 2009, pp. 533 –537.

[3] M. Lienard, M. Carrion, V. Degardin, and P. Degauque, "Modeling and Analysis of In-Vehicle Power Line Communication Channels," in *IEEE Trans. Veh. Technol.*, vol. 57, no. 2, Mar. 2008, pp. 670–679.

[4] M. Mohammadi, L. Lampe, M. Lok, S. Mirabbasi, M. Mirvakili, R. Rosales, and P. van Veen, "Measurement Study and Transmission for In-vehicle Power Line Communication," in *Proc. IEEE Intl. Symposium on Power Line Commun. and its Appl.*, Apr. 2009, pp. 73–78.

[5] V. Degardin, M. Lienard, P. Degauque, E. Simon, and P. Laly, "Impulsive Noise Characterization of In-Vehicle Power Line," *IEEE Electromagn. Compat.*, vol. 50, no. 4, pp. 861–868, Nov. 2008.

[6] D. Umehara, M. Morikura, T. Hisada, S. Ishiko, and H. Satoshi, "Statistical Impulse Detection of In-Vehicle Power Line Noise Using Hidden Markov Model," in *Proc. IEEE Intl. Symposium on Power Line Commun. and its Appl.*, Mar. 2010.

[7] Y. Yabuuchi, U. Daisuke, M. Morikura, T. Hisada, S. Ishiko, and S. Horihata, "Measurement and Analysis of Impulsive Noise on In-Vehicle Power Lines," in *Proc. IEEE Intl. Symposium on Power Line Commun. and its Appl.*, 2010.

[8] M. Tlich, G. Avril, and A. Zeddam, "Coherence bandwidth and its relationship with the RMS delay spread for PLC channels using measurements up to 100 MHz," *Home Networking*, vol. 256, pp. 129–142, 2008.

[9] A. Schiffer, "Statistical Channel and Noise Modeling of Vehicular DC-Lines for Data Communication," in *Proc. IEEE Veh. Technol. Conf.*, vol. 1, 2000, pp. 158–162.

[10] V. Degardin, M. Lienard, P. Degauque, and P. Laly, "Performances of the HomePlug PHY layer in the context of in-vehicle powerline communications," in *Proc. IEEE Intl. Symposium on Power Line Commun. and its Appl.*, Mar. 2007, pp. 93–97.